EXPERIMENTAL EVALUATION OF HIGH BANDWIDTH HELICOPTER FLIGHT CONTROL SYSTEM DESIGNS EXPLOITING ROTOR STATE FEEDBACK

J. Howitt
S.E. Howell
Defence Evaluation & Research Agency
Bedford, UK

P.R. Brinson
G.J. Mullen
University of Bristol
Bristol, UK

I.J. Woodrow
C. Hayhurst
GKN Westland Helicopters Ltd.
Yeovil, UK

Abstract

The continuing drive to extend the 24 hour, all-weather operational capabilities of helicopters is demanding more advanced flight control systems with higher levels of feedback gain to achieve the desired command tracking and disturbance rejection performance requirements. Achieving robust high gain feedback in helicopter flight control system design is problematic, however, because the rotor and fuselage are dynamically coupled in the frequency range of the desired closed-loop crossover, and the rotor thus becomes an integral part of the dynamic system that has to be controlled. The rotor system is also the dominant source of inter-axis coupling and dynamic uncertainty. The concept of Rotor State Feedback (RSF) is intended to augment conventional rigid-body feedback with measurements of the rotor dynamics to allow explicit and robust control of the coupled body/rotor modes at higher bandwidths than would otherwise be achievable. To this end, DERA, GKN Westland Helicopters and the University of Bristol have been conducting an experimental evaluation of RSF controllers using the University's Experimental Rotor Rig Facility and have also been applying modern multivariable controller design techniques to better exploit the additional degrees of freedom. The tests have included frequency sweeps and small, moderate and large amplitude step responses, with the results being related to full-scale in the context of ADS-33D flying qualities requirements. The programme has proven :

- The Rotor Rig exhibits coupled body/rotor dynamics and model uncertainty representative of the Westland Lynx
- The Rotor Rig provides a flexible environment for experimental testing of high bandwidth controllers.
- High bandwidth control requires RSF or sufficient dynamic compensation to estimate the rotor states.
- Up to a 50% increase in closed-loop bandwidth can be gained via RSF with respect to conventional limited authority rigid-body feedback.
- Robust performance is maintained in the presence of 30% on-axis model uncertainty and 100% off-axis model uncertainty.

It is thus concluded that the concept of Rotor State Feedback yields potentially significant advances in robust high bandwidth control.

Notation

$[A,B,C,0]$	=	system state space matrices
F, K	=	H_∞/Eigenstructure Assignment state feedback controller matrices
G	=	system transfer function matrix
H	=	H_∞ observer matrix
K_β	=	rotor blade flap stiffness (Nm)
I_β	=	rotor blade inertia (kg m^2)
I_{xx}, I_{yy}	=	roll/pitch moments of inertia (kg m^2)
R	=	rotor radius (m)
T	=	eigenvector matrix
W_1, W_2	=	compensator transfer function matrices
X, Z	=	positive definite solutions to Riccati equation
a_0	=	lift curve slope
c	=	rotor blade chord (m)
p, q	=	roll/pitch rate (rad s^{-1})
$\underline{x}$, $\underline{u}$, $\underline{y}$	=	system state, input and output vectors
Δ	=	perturbation matrix
Λ	=	diagonal matrix of eigenvalues
Ω	=	rotorspeed (rad s^{-1})
β_{1S}, β_{1C}	=	lateral/longitudinal flapping (rad)
ε	=	stability margin
ϕ, θ	=	roll/pitch attitude (rad)
γ	=	rotor Lock number
γ_{min}	=	robustness indicator
λ_β	=	blade flap frequency ratio
λ_{1C}, λ_{1S}	=	lateral/longitudinal inflow (m s^{-1})
λ_i	=	ith eigenvalue
v_i, w_i	=	ith right/left eigenvector
θ_{1C}, θ_{1S}	=	lateral/longitudinal cyclic pitch (rad)
ρ	=	air density (kg m^{-3})

Introduction

The continuing drive to extend the 24 hour, all-weather operational capabilities of helicopters is demanding advanced flight control systems with flying qualities tailored appropriately for the mission task. By reducing pilot workload and allowing safe use of the full performance envelope, there is significant potential for improved mission effectiveness, particularly when required to operate in degraded environmental conditions. Providing optimum flying qualities is generally considered to be best achieved through application of full authority Fly-By-Wire (FBW) or Active Control Technology (ACT), exploiting high levels of feedback gain to achieve the desired command tracking and disturbance rejection performance requirements.

The Challenge of High Bandwidth Flight Control

The application of FBW/ACT to helicopters has tended to lag noticeably behind the technology exploitation on fixed wing programmes. This is partly due to perceived economic constraints, but is equally related to engineering design and qualification considerations.

Achieving robust high gain feedback in helicopter flight control system design is problematic because the rotor and fuselage are dynamically coupled in the frequency range of the desired closed-loop crossover, and the rotor thus becomes an integral part of the dynamic system that has to be controlled. The rotor system is also the dominant source of inter-axis coupling and dynamic uncertainty. To this end, the concept of Rotor State Feedback (RSF) (Refs. 1 - 3) is intended to augment conventional rigid-body feedback with measurements of the rotor dynamics to allow explicit and robust control of the coupled body/rotor modes at higher bandwidths than would otherwise be achievable.

UK Innovation in Helicopter Flight Control

To advance the appreciation of closed-loop coupled body/rotor control, the University of Bristol has developed an Experimental Rotor Rig Facility (ERRF) with a programmable full-authority FBW control system that enables new and novel controller designs to be tested in a representative dynamic environment. The Rig has formed the key element in a joint DERA, GKN Westland Helicopters and University of Bristol research programme on the "Experimental Evaluation of Control System Design Techniques for Helicopters". The aim of this programme has been twofold :

- to apply modern multivariable design techniques to the helicopter flight control problem and build confidence in the effectiveness and integrity of such techniques.

- to demonstrate the potential of RSF for robust, high bandwidth control

Through experimental testing, the longer term goal is to minimise the risk associated with such innovation and to ensure that its benefits find effective application in UK industry.

Motivation for use of Rotor State Feedback

A useful insight into the motivation for RSF can be gained by examining simple feedback theory. Consider the trace of the open- and closed-loop system matrices, A, where the trace is the sum of the diagonal elements and can also be shown to be equal to the sum of the eigenvalues :

$$trace(A) = \sum_{i=1}^{n} A_{ii} = \sum_{i=1}^{n} \lambda_i \qquad (1)$$

For the closed-loop system described by $A_{cl} = (A - BKC)$, where K is a feedback controller of the form $\underline{u} = -K\underline{y}$:

$$trace(A - BKC) = trace(A) - trace(BKC) \qquad (2)$$

For systems where $CB = 0$ (*i.e.* none of the control inputs is a direct forcing function on any of the feedback states) :

$$trace(BKC) = 0 \Rightarrow trace(A - BKC) = trace(A) \qquad (3)$$

and the sum of the open- and closed-loop eigenvalues must be equal. This is true for any closed-loop helicopter flight control system design that uses only rigid-body feedback - *e.g.* earth-referenced attitudes and/or body-referenced rates.

Hence, if the flying qualities requirements dictate that the poles associated with the closed-loop rigid-body modes be moved further into the left-half plane than the corresponding open-loop modes, then the poles associated with the closed-loop rotor modes must move an equivalent amount toward the right-half plane - *i.e.* destabilising. The bandwidth of the closed-loop rigid body system is thus limited by stability constraints on the rotor modes.

When using rotor state feedback - *e.g.* shaft-referenced flap and lag angles - it can be shown that the cyclic pitch control inputs act as direct forcing functions on the right-hand side of the rotor state equations and that consequently $CB \neq 0$. With reference to Eqn. 2, the control system designer thus has far greater freedom over the closed-loop eigenstructure and can modify the dynamic behaviour of the rigid body and rotor modes independently of one another.

Rotor state feedback can therefore be seen to be an important element of any high bandwidth controller, or, alternatively, the controller must include sufficient dynamic compensation to allow the rotor states to be estimated.

Scope of the Paper

To set the experimental analysis of RSF controllers in context, data are presented that relate the dynamic characteristics of the Rotor Rig - and the associated design model - to those of a full-scale helicopter, namely the Westland Lynx.

The paper then presents a detailed discussion of the implicit RSF properties of an output feedback H_∞ controller (optimised in the frequency domain for robustness to model uncertainty) and the explicit RSF properties of a full state feedback Eigenstructure Assignment controller (optimised in the time domain for flying qualities). Results for a simple SISO PID rigid-body controller are also included for comparison.

Finally, the behaviour of the closed-loop systems are expressed in terms of compliance with ADS-33D flying qualities requirements (Ref. 4).

Description Of The Experimental Rotor Rig

A comprehensive description of the University of Bristol Experimental Rotor Rig Facility (Fig. 1) can be found in Ref. 5, but a brief overview is given below.

The Rig consists of a four bladed 1.5m diameter rotor, with rigid hub and 60mm chord, Gottingen 436 section, GRP rotor blades (from the ML Aviation Sprite UAV), driven at 1500rpm. The rotor system is gimballed to provide pitch and roll degrees of freedom up to approximately 40° attitude, but is fixed in yaw and all translational axes. A unique feature of the Rig is its high performance actuation system. This comprises brushless DC motors connected to a conventional swashplate system, providing blade pitch slew rates in excess of 800° s^{-1} at the blade root and a small amplitude signal bandwidth exceeding 50 Hz.

Incremental shaft encoders provide accurate measurements of actuator positions, rotor blade azimuth position and pitch and roll attitudes. Individual flap angles are derived from blade mounted strain gauge measurements which are passed down through a slip ring assembly.

The complete Rotor Rig assembly is mounted in the return section of the University of Bristol large wind tunnel and can be tested up to an advance ratio of $\mu = 0.08$ (equivalent to airspeeds of approximately 35 knots at full-scale). The control of the Rig is fully computerised and the system software contains extensive built in safety monitoring.

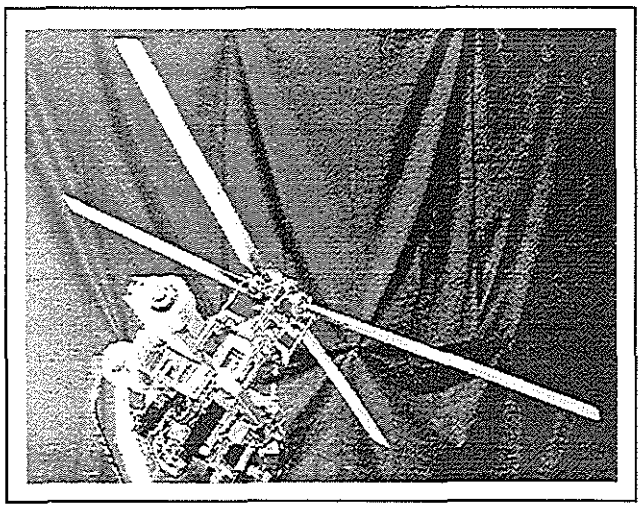

Figure 1
The University of Bristol Experimental Rotor Rig Facility

The Rotor Rig has been designed such that the ratio of pitch/roll moment per unit flapping to rigid body inertia, normalised with respect to the square of rotorspeed, (denoted by *C*, Ref. 6), is typical of a modern hingeless rotor.

Table 1 presents a comparison of these ratios for the Rotor Rig, the stiff hingeless rotor of the Westland Lynx and the articulated rotor of the Eurocopter Puma.

Table 1
Comparison of normalised ratios of pitch/roll moment per unit flapping to rigid body inertia

Type	C_{pitch}	C_{roll}
Rotor Rig	0.0297	0.1055
Westland Lynx	0.0214	0.1076
Eurocopter Puma	0.0083	0.0285

The ratios for the Rotor Rig compare favourably with Lynx, particularly in roll, and are an order of magnitude greater than the respective values for the Puma. This design feature ensures that the Rig reproduces the fundamental character of coupled body/rotor behaviour for high bandwidth hingeless rotors.

Description of the Flight Mechanics Design and Simulation Model

An appreciation of the fundamental dynamics of rotor blade flapping is key to understanding the stability and control of the coupled body/rotor system. The sections below detail the manner in which blade flapping is embodied within the DERA HELISIM flight mechanics model (Ref. 7), the form of the model used for design, analysis and simulation of RSF controllers for the Rotor Rig, and a comparison of the validity of the model - in terms of dynamic uncertainty - with respect to full-scale.

Stability and Control Issues Relating to Blade Flapping

Consider the flapping dynamics of a hovering rotor of radius R, blade chord c, lift slope a_0, flap stiffness K_β, and blade inertia I_β rotating at Ω rad s^{-1}. A detailed derivation of the modal dynamics in non-rotating multi-blade co-ordinates can be found in Ref. 7. Briefly, the coning mode is an independent, decoupled degree of freedom, whereas the longitudinal and lateral cyclic flap degrees of freedom are coupled and can be expanded as :

$$\ddot{\beta}_{1C} + n_\beta \dot{\beta}_{1C} + \left(\lambda_\beta^2 - 1\right)\beta_{1C} + 2\dot{\beta}_{1S} + n_\beta \beta_{1S} = 2(\bar{p} + \dot{\bar{q}}/2) + n_\beta\left[\theta_{1C} + (\bar{q} - \lambda_{1C})\right] \quad (4)$$

$$\ddot{\beta}_{1S} + n_\beta \dot{\beta}_{1S} + \left(\lambda_\beta^2 - 1\right)\beta_{1S} - 2\dot{\beta}_{1C} - n_\beta \beta_{1C} = -2(\bar{q} - \dot{\bar{p}}/2) + n_\beta\left[\theta_{1S} + (\bar{p} - \lambda_{1S})\right] \quad (5)$$

where,

$(\lambda_\beta^2 - 1) = K_\beta / I_\beta \Omega^2$
$\gamma = \rho c a_0 R^4 / I_\beta$
$n_\beta = \gamma / 8$
$\bar{p} = p / \Omega$
$\bar{q} = q / \Omega$

It can also be shown that the eigenvalues of the cyclic flapping system (non-dimensionalised with respect to Ω) are the roots of the characteristic equation :

$$\left(\lambda^2 + (\gamma/8)\lambda + \lambda_\beta^2 - 1\right)^2 + \left(2\lambda + \gamma/8\right)^2 = 0 \qquad (6)$$

With reference to Fig. 2, the system is described by an advancing flap mode ($\lambda = \lambda_\beta + 1$) and a regressing flap mode ($\lambda = \lambda_\beta - 1$).

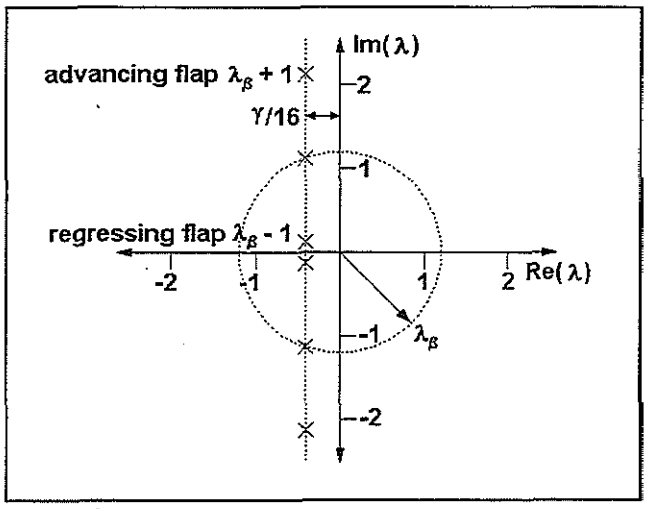

Figure 2
Eigenvalues of the multi-blade co-ordinate flapping system

The regressing flap mode frequency is of a similar order of magnitude to the highest frequency fuselage modes and can couple to form complex modes. It is these coupled body/rotor modes that dominate the dynamic response of the helicopter in the frequency range of the desired closed-loop crossover when seeking to achieve robust high bandwidth control.

For a rotor with N_b blades, the roll and pitch hub moments, L and M, resulting from out-of-plane flapping are proportional to the rotor stiffness, K_β :

$$L = \frac{-N_b K_\beta \beta_{1S}}{2} \qquad (7)$$

$$M = \frac{-N_b K_\beta \beta_{1C}}{2} \qquad (8)$$

The roll and pitch accelerations, p and q, can then be approximated by :

$$\dot{p} = \frac{L}{I_{xx}} \qquad (9)$$

$$\dot{q} = \frac{M}{I_{yy}} \qquad (10)$$

where, I_{xx} and I_{yy} are the roll and pitch moments of inertia respectively.

The in-plane lag dynamics have a similar form to the flapping dynamics, and there are equivalent advancing and regressing lag modes. At full-scale, these modes tend to be weakly damped - even with the addition of mechanical dampers - and hence, although they do not contribute significantly to the control of the helicopter in the manner of the flapping modes, they are equally susceptible to destabilisation by high gain feedback (Ref. 8) and need to be included in any flight mechanics analysis. In the context of the Rotor Rig, however, the rotor is very stiff in lag and coupling with the fuselage dynamics does not occur. Modelling of the lag modes was thus ignored for the purposes of this study.

Form of the Design, Analysis and Simulation Model

The mathematical model of the Rotor Rig is based upon the generic DERA HELISIM flight mechanics model (Ref. 7), configured with appropriate aerodynamic, dynamic and inertial data. From this, a small perturbation state-space linear model was generated about a hover trim condition for the purpose of controller design, analysis and simulation :

$$\begin{aligned} \dot{\underline{x}} &= A\underline{x} + B\underline{u} \\ \underline{y} &= C\underline{x} \end{aligned} \qquad (11)$$

where,

$$\underline{x} = \left[\theta, \phi, q, p, \beta_{1C}, \beta_{1S}, \dot{\beta}_{1C}, \dot{\beta}_{1S}\right]^T$$

$$\underline{u} = \left[\theta_{1Sdem}, \theta_{1Cdem}\right]^T$$

Actuator dynamics were ignored, since their bandwidth (400 rad s^{-1}) is more than an order of magnitude greater than the desired closed-loop attitude bandwidth. Actuator dynamics and saturation characteristics were included, however, for all closed-loop simulation. A modal decomposition for the system is detailed in Table 2.

Table 2
Frequency and damping of Rotor Rig open-loop modes

Mode	Frequency (rad/s)	Damping
Pitch/roll attitude	0.0	-
Pitch / flap	17.1	0.88
Roll / flap	41.4	0.54
Advancing flap	330.5	0.11

Note that both fuselage modes couple with the rotor. A coupled pitch/flap mode is not a feature of Lynx, since - with reference to Table 1 - the normalised ratio of moment per unit flapping to rigid body inertia is 50% lower than the Rig. For this reason, and also for brevity, the results presented in the remainder of this paper shall relate to the roll axis only.

Characterisation of Model Uncertainty

Having demonstrated previously that the coupled body/rotor dynamic behaviour of the Rotor Rig is representative of the Westland Lynx, it is instructive to compare the relative uncertainties of the associated HELISIM Rotor Rig and Lynx models.

Uncertainty can be calculated in the complex frequency domain as :

$$\Delta(j\omega) = \frac{\left| G_{expt}(j\omega) - G_{model}(j\omega) \right|}{\left| G_{model}(j\omega) \right|} \qquad (12)$$

The experimental frequency response data for the Lynx is derived from frequency sweeps conducted in flight on DERA Lynx ZD559 (Mk. 7, metal blades, autostabilisation engaged) in the hover. Similar frequency sweeps were also conducted on the Rotor Rig. In both cases the model data were calculated analytically from linear HELISIM models of the Lynx and Rotor Rig respectively.

Figure 3 presents the on-axis (roll attitude) and off-axis (pitch attitude) uncertainty to lateral cyclic control inputs with the solid line denoting the Rotor Rig and the dashed line denoting the Lynx. Note also that the frequency scale has been normalised with respect to rotorspeed for means of comparison.

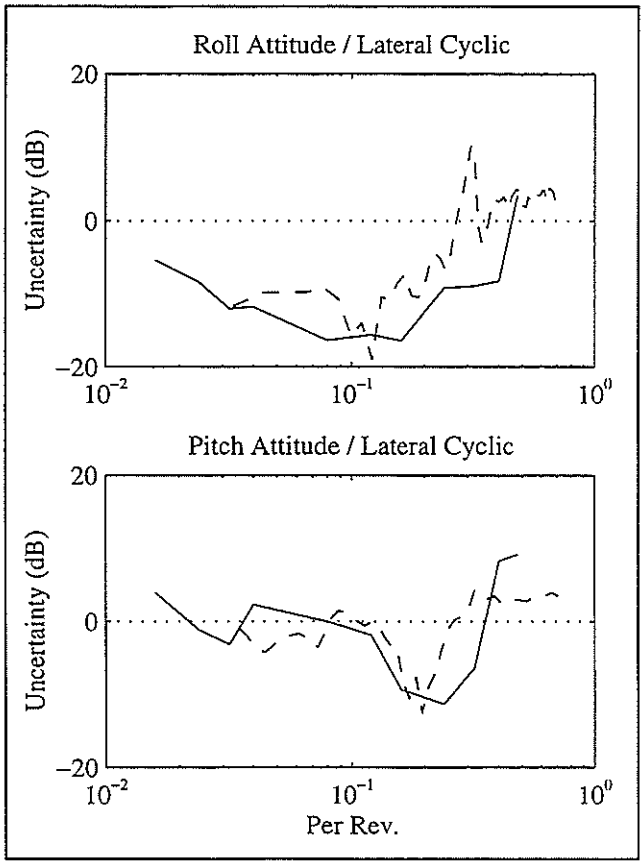

Figure 3
Characterisation of HELISIM Rotor Rig and Lynx model uncertainties to roll axis control inputs

The on-axis uncertainty for both systems is generally low, typically less than 30% (-10dB) across all frequencies below 0.2Ω, but rises significantly in the region of the coupled roll/flap mode, 0.3Ω - 0.5Ω, where uncertainty exceeds 100% (0dB). Off-axis uncertainty, however, is of the order of 100% across all frequencies - *i.e.* even the sign of the off-axis response is in error - and presents a significant robustness problem for any closed-loop control system.

It should be noted, again, that the characteristics of the Rotor Rig are very similar to those of the Lynx and that one can assume reasonable confidence in the read-across of the performance and robustness properties of the Rotor Rig RSF controllers to full-scale.

Design Requirements

A basic functional requirement dictated that the RSF controllers should :

i) provide an attitude command, attitude hold (ACAH) response type in both pitch and roll

ii) operate within the computational frame time of 1ms

iii) operate within the cyclic amplitude limits of ±6° and rate limits of ±800° s^{-1}

In designing a feedback controller, one would seek to close the loop around the fuselage attitudes with sufficient gain to achieve good command tracking and disturbance rejection properties, maintain (or increase) the damping of the coupled body/rotor modes, and decouple the roll and pitch axes. The chosen performance requirements were based on ADS-33D criteria (Ref. 4), the current US Army Aviation Systems Command specification detailing the requirements for the flying qualities of military rotorcraft. This document was adopted for evaluation of control systems on the Experimental Rotor Rig Facility in order to facilitate comparison between the Rig and application at full-scale.

Evidently, the requirements for the Rig need to be modified for read across to full-scale, and hence it is appropriate to again normalise with respect to rotorspeed. With reference to the Lynx, the ratio of rotorspeeds is given by $\Omega_{Rig}/\Omega_{Lynx} \approx 4.4$. Table 3 thus defines the equivalent roll attitude bandwidths, at full-scale and scaled for the Rig, for :

- ADS-33D Level 1 flying qualities
- Lynx (flight test data)
- Rig (open-loop, measured experimentally)
- Rig closed-loop design requirements

These data were calculated for both pitch and roll axes, but, again for brevity, only the roll axis data are presented. With reference to Table 3, the primary closed-loop design goal was taken to be an equivalent ADS-33D attitude bandwidth of approximately 150% of the open-loop value.

Table 3
Definition of closed-loop performance targets with respect to full-scale flying qualities requirements

Roll Axis	Full-Scale	Rig-Scale
ADS-33D L1 (target track)	2.5	11.0
Lynx (flight test approx.)	4.7	20.7
Rig (open-loop, measured)	5.1	22.5
Rig (closed-loop target)	7.5	33.0

Whilst this design target may be significantly higher than required for the primary response to pilot control inputs, the additional performance offers the potential for significant advances in robust command tracking and disturbance rejection, particularly when implementing the controller in a two degree-of-freedom explicit model following architecture (Ref. 9).

An additional design goal was to decouple the primary responses. Again applying normalised ADS-33D criteria, the requirement was for the ratio of peak off-axis response from trim within 0.9 seconds (4.0 seconds at full-scale) to the desired on-axis response from trim at 0.9 seconds, $\Delta\phi_{pk}/\Delta\theta_{0.9}$ or $\Delta\theta_{pk}/\Delta\phi_{0.9}$, following an abrupt control step input to be less than 25%.

Overview Of Multivariable Design Techniques

Detailed below is an overview of the H_∞ and Eigenstructure Assignment multivariable synthesis techniques that were applied to the design of RSF controllers for the Rotor Rig.

An Overview of H_∞ Loop Shaping Synthesis

The H_∞ Loop Shaping controller design technique (Refs. 10 - 12) is a frequency domain method that describes uncertainty in terms of additive perturbations of a normalised coprime factorisation of the system.

The ongoing experimental study of controller design techniques on the Rotor Rig (Ref. 13) has shown that H_∞ rigid-body output feedback controllers exhibit superior performance and robustness properties to other multivariable controllers of similar structure. Indeed, expressing the controllers in observer state feedback form - as one can for all linear time invariant controllers - reveals that the use of observable rotor dynamics within the feedback augmentation is unique to the H_∞ controller. Thus, whilst based on rigid-body output feedback, the use of rotor state feedback is in fact implicit within the H_∞ synthesis. The method is also of particular interest when considering application to the Rotor Rig because it seeks to capture robustness to model uncertainty within the design process.

Consider the system $G = [A,B,C,0]$ with a normalised left coprime factorisation $G = M^{-1}N$ such that the uncertainty can be described by :

$$G_{pet} = \left(M + \Delta_M\right)^{-1}\left(N + \Delta_N\right) \tag{13}$$

where G_{pet} is the perturbed system model and Δ_M and Δ_N are stable unknown transfer functions as shown in Fig. 4 :

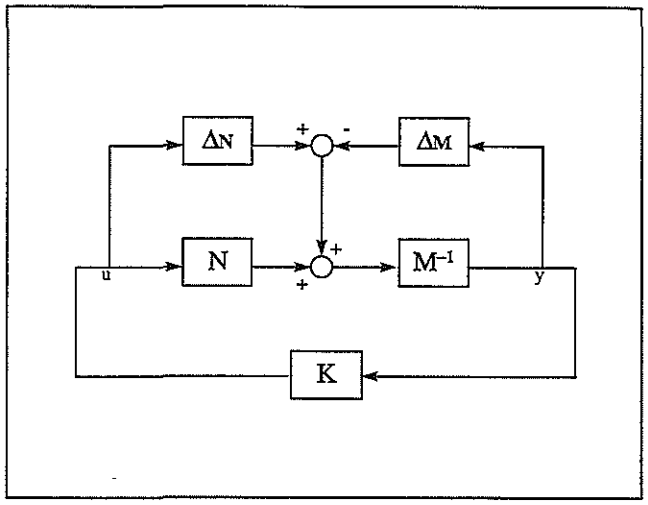

Figure 4
Robust stabilisation problem

With reference to Fig. 4, the H_∞ control problem can be summarised as :

$$G_{pet} = \left\{\left(M + \Delta_M\right)^{-1}\left(N + \Delta_N\right) : \left\|\Delta_M, \Delta_N\right\|_\infty < \varepsilon\right\} \tag{14}$$

where the objective is to find the largest family of perturbed systems - *i.e.* ε_{max} - for which closed loop stability can be conferred by a single fixed controller K. The maximum stability margin, ε_{max}, is given by the minimisation of :

$$\varepsilon_{max}^{-1} = \gamma_{min} = \inf_K \left\| \begin{bmatrix} K \\ I \end{bmatrix} (I - GK)^{-1} M^{-1} \right\|_\infty \tag{15}$$

In this form, the H_∞ synthesis does not accommodate classical frequency dependent performance requirements. This can be accounted for, however, by application of a pre-compensator, W_1, and a post-compensator, W_2 in series with the system :

$$G_s = W_2 G W_1 \tag{16}$$

Thus typical performance objectives of high gain at low frequency, to ensure good command tracking, and low gain at high frequency, to ensure good noise rejection, can be specified through appropriate shaping of W_1 and W_2. The gain of W_1 and W_2 can also be used to assign closed-loop system bandwidth through modification of the open-loop 0dB crossover.

A trade-off exists between the performance that can be achieved via application of W_1 and W_2, and the stability robustness that can be achieved from submitting the shaped system to the H_∞ Synthesis. To this end, the γ_{min} metric provides the designer with an indicator of the compatibility of the open-loop singular values with closed-loop stability robustness. A value of $\gamma_{min} < 4$ is typically sought (Ref. 11), although a sub-optimal $\gamma > \gamma_{min}$ is often chosen to avoid introducing overly fast poles into the controller.

For a minimal state-space realisation of the shaped system, $G_s = [A_s, B_s, C_s, 0]$, the optimal γ and controller can be calculated by solution of the Control Algebraic Riccati Equation and Filtering Algebraic Riccati Equation :

$$\begin{aligned} A_s^* X + X A_s - X B_s B_s^* X + C_s^* C_s = 0 \\ A_s Z + Z A_s^* - Z C_s^* C_s Z + B_s B_s^* = 0 \end{aligned} \tag{17}$$

It can also be shown (Ref. 10) that the controller can be expressed as an observer plus state feedback controller:

$$\begin{aligned} \dot{\hat{x}} &= A_s \hat{x} + H\left(C_s \hat{x} - y\right) + B_s u \\ u &= F\hat{x} \end{aligned} \tag{18}$$

Where H is the observer matrix and F the fixed gain state feedback controller matrix given by :

$$H = -Z C_s^* \tag{19}$$

$$F = B_s^T \left(\gamma^{-2} I + \gamma^{-2} XZ - I\right)^{-1} X \tag{20}$$

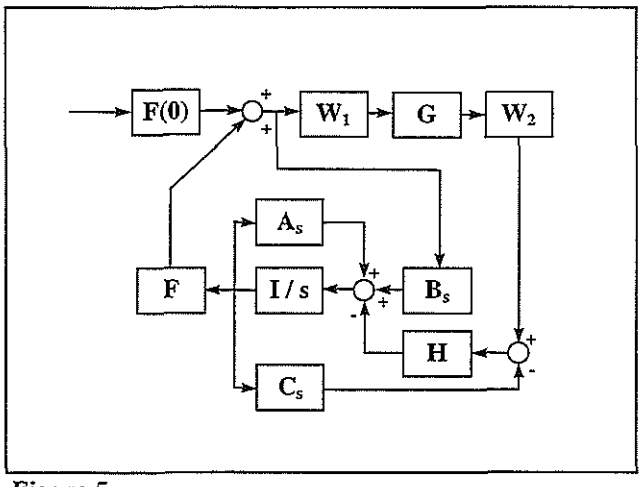

Figure 5
Observer implementation of H_∞ loop shaping controller

An Overview of Eigenstructure Assignment

Although Eigenstructure Assignment (Ref. 14) does not expressly capture robustness constraints in the manner of H_∞ synthesis, it was chosen for this application because the method does allow a high degree of visibility into the underlying vehicle dynamics. In particular, it executes control in a modal manner, hence allowing explicit regulation of the coupled body/rotor modes.

For the state-space, linear time-invariant system :

$$\begin{aligned} \dot{\underline{x}} &= A\underline{x} + B\underline{u} \\ \underline{y} &= C\underline{x} \end{aligned} \tag{21}$$

The state matrix A can be expressed in modal form, thus :

$$A = T\Lambda T^{-1} \tag{22}$$

such that the eigenvalues λ_i form the principal diagonal of Λ, the columns of T are the right eigenvectors v_i, and the rows of T^{-1} are the left eigenvectors w_i^T that satisfy :

$$\left[\lambda_i I - A\right] v_i = w_i^T \left[\lambda_i I - A\right] = 0 \tag{23}$$

It can be shown (Ref. 14), that the dynamic response of the system to a command or disturbance input depends on :

- the eigenvalues, which determine the damping and frequency of each mode,
- the right eigenvectors, which determine the states participating in each modal response,
- the left eigenvectors, which determine the states excited by each input.

It is evident that the application of feedback will modify the eigenvalues and right eigenvectors and that feedforward can be used to modify the left eigenvectors. Including a linear feedback controller :

$$\underline{u} = -K\underline{y} \tag{24}$$

results in the closed-loop state equation :

$$\dot{\underline{x}} = (A - BKC)\underline{x} \tag{25}$$

For an m input, p output system, the Eigenstructure Assignment problem is thus to formulate the gain matrix K such that the eigenvalues λ_i *(i=1,2, ... n)* and the associated eigenvectors $\underline{v_i}$ of *(A - BKC)* are in some way optimal within the constraints that *(i)* no more than p eigenvalues can be chosen arbitrarily, and *(ii)* no more than m entries in any one eigenvector can be chosen arbitrarily. Obviously, the greater the number of independent control inputs and state measurements, the greater the freedom in the design process. Note also that the left eigenvectors are fixed for a given feedback controller, but that a feedforward controller K_{ff} can be used to give a design freedom over the closed-loop B matrix and hence modify the input coupling (Ref. 15). The resulting closed-loop system is now described by :

$$\dot{\underline{x}} = (A - BKC)\underline{x} + BK_{ff}\underline{r} \tag{26}$$

where, $\underline{r}$ is the m dimensional reference input.

Discussion Of Controller Designs

Detailed below is an review of the RSF controllers resulting from application of the H_∞ and Eigenstructure Assignment techniques to the Rotor Rig. Details of a simple SISO PID rigid-body feedback controller are also presented for comparison.

H_∞ Loop Shaping RSF Controller

The output feedback H_∞ loop-shape RSF controller was designed around the two input, two output linear model :

$$\begin{aligned} \dot{\underline{x}} &= A\underline{x} + B\underline{u} \\ \underline{y} &= C\underline{x} \end{aligned} \tag{27}$$

where,

$$\underline{x} = \left[\theta, \phi, q, p, \beta_{1C}, \beta_{1S}, \dot{\beta}_{1C}, \dot{\beta}_{1S}\right]^T$$
$$\underline{u} = \left[\theta_{1Sdem}, \theta_{1Cdem}\right]^T$$
$$\underline{y} = \left[\theta, \phi\right]^T$$

Examination of the open-loop singular values indicated that integral action was required to increase the low frequency gain and improve command tracking. In order to prevent excess high frequency phase lag, this was implemented as a proportional plus integral pre-filter with zeros at 5 and 10 rad s^{-1} for the pitch and roll axes respectively. An additional pre-multiplying gain was also specified to give open-loop 0dB crossover frequencies commensurate with the desired closed loop bandwidths. The resulting W_1 pre-filter was :

$$W_1 = \begin{bmatrix} \dfrac{0.49(s+5)}{s} & 0 \\ 0 & \dfrac{1.25(s+10)}{s} \end{bmatrix} \tag{28}$$

The high frequency roll-off of the open-loop singular values was deemed to give satisfactory noise rejection characteristics and hence the post-filter W_2 was simply :

$$W_2 = \begin{bmatrix} 1 & 0 \\ 0 & 1 \end{bmatrix} \tag{29}$$

The robustness indicator for the augmented system, $G_s = W_2GW_1$, was calculated to be $\gamma_{min} = 2.59$, which indicates that the specified loop shapes are compatible with robust stabilisation. The augmented system was therefore submitted to the H_∞ Synthesis, and the exact observer and state feedback gain matrices were calculated for a sub-optimal $\gamma = 1.1 * \gamma_{min}$.

The state feedback gain matrix (expressed in terms of deg. blade angle demand per deg. or deg. s^{-1} of system response) is given in Table 4.

Table 4
H_∞ Loop Shaping state feedback controller gains

	θ_{1s}	θ_{1c}
$\int\theta$	-4.2520	-0.1126
$\int\phi$	-0.1437	-8.5234
θ	-0.9958	0.1091
ϕ	0.0765	0.9958
q	-0.0828	0.0128
p	0.0116	0.0330
β_{1c}	0.7078	0.0803
β_{1s}	-0.1617	-0.9079
$\dot{\beta}_{1c}$	0.0001	-0.0026
$\dot{\beta}_{1s}$	-0.0022	-0.0010

Note the strong diagonal dominance between corresponding pairs of feedback signals and the significant level of flap angle feedback required to achieve the necessary phase advance compensation for robust stability. The modal decomposition of the resulting closed-loop system is given in Table 5.

Table 5
Frequency and damping of H_∞ closed-loop system modes

Mode	Frequency (rad/s)	Damping
∫ Pitch Attitude	5.4	1.00
∫ Roll Attitude	10.6	1.00
Pitch/Roll ?	11.9	0.84
Pitch/Flap ?	20.7	0.83
Roll/Flap	42.6	0.51
Advancing Flap	330.5	0.11

By observation of the associated eigenvectors, it is evident that the H_∞ Synthesis retains the open-loop characteristics of both the advancing flap and the coupled roll/flap mode. The coupled pitch/flap mode is no longer clearly identifiable, however, having further coupled with the real pitch and roll attitude modes. The two new complex modes, at approximately 12 and 21 rad s^{-1}, are markedly different in character. Whilst the H_∞ Synthesis achieves significant robustness, it is a disadvantage that the resulting closed-loop system cannot be interpreted in terms of the classical characteristic modes. This impacts on the ability to relate the closed-loop performance to the design specification and mitigates against refinement of the controller.

Herein lies the appeal of Eigenstructure Assignment, whereby the closed-loop dynamics can be addressed directly through specification of the modal characteristics.

Eigenstructure Assignment RSF Controller

The Eigenstructure Assignment controller was designed from the outset to feature full state feedback including measurements of the rotor flapping states. Unfortunately, these signals proved to be prone to noise and drop-outs, and were therefore considered unsuitable for use within a feedback controller, particularly where derivatives of the flap angle were required. It was therefore deemed necessary to reconstruct the blade flapping information using a state estimator. In this case, the same H_∞ observer matrix, H, was used to provide state estimation for the Eigenstructure Assignment controller, K, and a direct substitution for the H_∞ controller, F, was made in the feedback system described by Fig. 5. Although the lack of rotor state measurement was a disappointment, this common implementation did allow a direct comparison between the implicit RSF properties of the output feedback H_∞ Loop Shaping controller and the explicit RSF properties associated with full state feedback Eigenstructure Assignment. To this end, the Eigenstructure Assignment controller was designed around the same P+I augmented open-loop system, $G_s = W_2GW_1$.

The objective was to achieve similar performance and robustness to the H_∞ design, but to maintain the underlying visibility associated with the classical modal structure. Thus the closed-loop eigenstructure was specified to map directly the open-loop eigenstructure of the complex rotor modes - since this was seen in the H_∞ Synthesis to give good robustness - whilst optimising the real eigenvalues and eigenvectors associated with the rigid-body modes. The resulting state feedback gain matrix is given in Table 6.

Table 6
Eigenstructure Assignment state feedback controller gains

	θ_{1s}	θ_{1c}
$\int\theta$	-3.7119	-0.4585
$\int\phi$	-0.4223	-9.5716
θ	-1.1263	0.2323
ϕ	-0.3153	0.6787
q	-0.1233	0.0167
p	0.0067	0.0449
β_{1c}	1.0914	-0.2062
β_{1s}	0.0996	-0.6544
$\dot{\beta}_{1c}$	0.0011	-0.0021
$\dot{\beta}_{1s}$	-0.0032	0.0002

As with the H_∞ controller, note the strong diagonal dominance between corresponding pairs of feedback signals and the significant level of flap angle feedback required to achieve the necessary phase advance compensation for robust stability. Note also that higher off-axis feedback is required to maintain the classical modal structure.

The modal decomposition of the resulting closed-loop system - again excluding observer and actuator dynamics - is given in Table 7. Note that all the classical modes have been retained.

Table 7
Frequency and damping of Eigenstructure Assignment closed-loop system modes

Mode	Frequency (rad/s)	Damping
∫ Pitch Attitude	6.0	1.00
∫ Roll Attitude	10.7	1.00
Pitch Attitude	9.8	1.00
Roll Attitude	16.4	1.00
Pitch / Flap	17.1	0.88
Roll / Flap	41.4	0.54
Advancing Flap	330.5	0.11

Classical SISO PID Rigid-Body Feedback Controller

For comparison with the two multivariable RSF controllers, a classical SISO PID rigid-body feedback controller was also designed around the same P+I augmented open-loop system. Taking the H_∞ controller as a starting point, all flap, flap rate and off-axis rigid-body gains were set to zero and the remaining three terms (effectively PID) were then re-optimised such that the on-axis closed-loop frequency responses matched the on-axis H_∞ closed-loop frequency responses in a least squares manner. The resulting state feedback gain matrix is given in Table 8.

Table 8
PID state feedback controller gains

	θ_{1s}	θ_{1c}
$\int\theta$	-4.5394	0
$\int\phi$	0	-6.9415
θ	-0.8646	0
ϕ	0	0.7104
q	-0.0699	0
p	0	0.0252

The modal decomposition of the resulting closed-loop system is given in Table 9. Note that the damping of the closed-loop coupled body/rotor modes have been eroded by approximately 50% (with respect to the open-loop values) in order to achieve the same rigid-body attitude bandwidths as the RSF closed-loop systems. This may be expected to cause stability problems experimentally.

Table 9
Frequency and damping of PID closed-loop system modes

Mode	Frequency (rad/s)	Damping
∫ Pitch Attitude	5.2	1.00
∫ Roll Attitude	8.3	1.00
Pitch/Roll ?	10.2	0.90
Pitch/Flap ?	21.7	0.58
Roll/Flap	45.3	0.31
Advancing Flap	328.7	0.11

Presentation Of Results

The following sections detail the results of the experimental testing of the H_∞ and Eigenstructure Assignment RSF controllers and the PID rigid-body closed-loop system. Testing was conducted in both the time and frequency domain and results are related to full-scale in the context of ADS-33D flying qualities requirements.

Time Domain

The time domain performance of each controller was investigated through the application of a series of roll attitude step demands of increasing net amplitude, ranging from 5° to 30°. For comparison, the lateral cyclic test signal was also applied to the non-linear closed-loop simulation models (Fig 7). In each case, the solid lines denotes the experimental response and the dashed lines denote the corresponding simulation model responses.

For both H_∞ and Eigenstructure Assignment RSF closed-loop systems, the on-axis experimental performance matches the simulation model very closely, indicating a high degree of robustness to model uncertainty, although both exhibit slightly less damping than predicted. The further reduction in damping suffered by the PID rigid-body closed-loop system is also apparent. For larger amplitude inputs - during which actuator saturation occurs and integrator anti-windup is implemented - both stability and command tracking are retained, but the amplitude of the overshoots is slightly increased. It is postulated that on-axis damping could be improved by including dynamic inflow effects within the design model, and that performance could be further enhanced by implementing each controller in a two degree-of-freedom explicit model following architecture.

Simulation suggests that very low cross-coupling should be associated with all the controllers, but - given the large off-axis model uncertainty - the experimental results show significant differences between the methods.

Relating the results to ADS-33D requirements, the peak off-axis response for the H_∞ RSF closed-loop system was $\Delta\theta_{pk}/\Delta\phi_{0.9} = 0.19$, for the Eigenstructure Assignment RSF closed loop system $\Delta\theta_{pk}/\Delta\phi_{0.9} = 0.14$ and for the PID rigid-body closed-loop system $\Delta\theta_{pk}/\Delta\phi_{0.9} = 0.31$. Hence, only the RSF controllers meet the desired performance requirements ($\Delta\theta_{pk}/\Delta\phi_{0.9} < 0.25$).

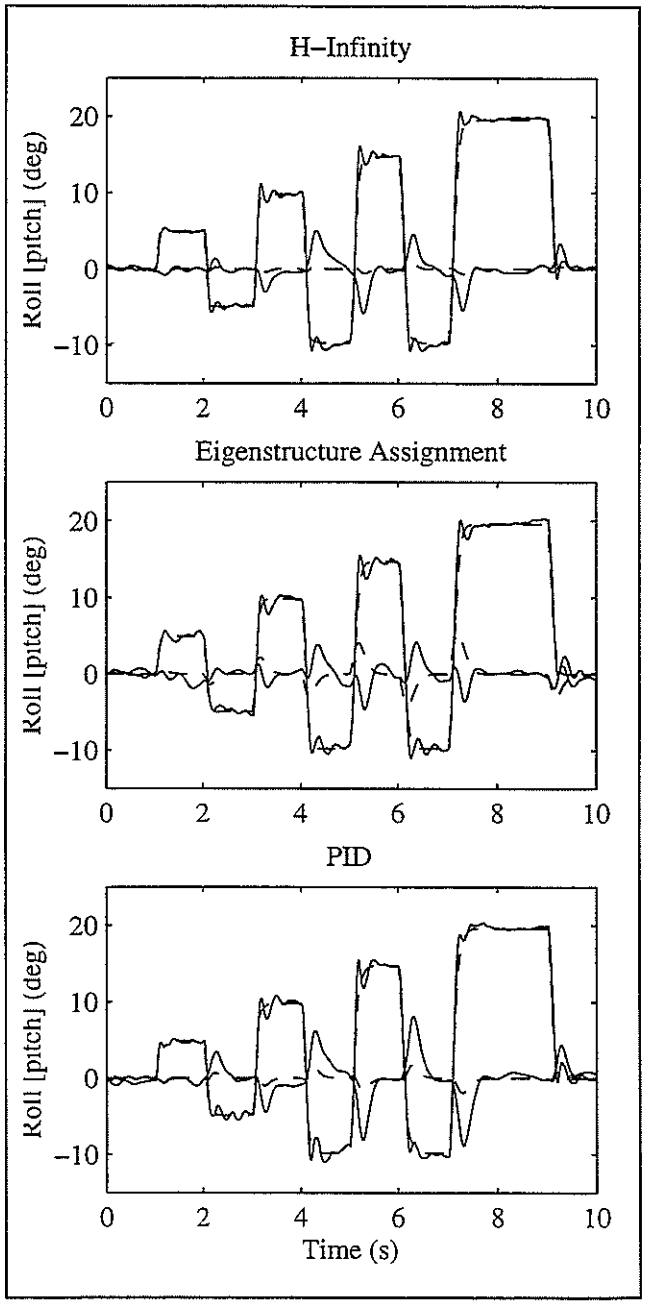

Figure 6
Comparison of experimental (solid) and modelled (dashed) time responses for H_∞, Eigenstructure Assignment and PID closed-loop systems to a series of attitude step demands of increasing net amplitude

Frequency Domain

Figure 8 presents the resulting Bode magnitude plots, with the closed-loop simulation model responses overlaid for comparison. Again, the solid line denotes the experimental response and the dashed lines denote the corresponding simulation model responses.

As with the time domain data, the on-axis experimental data match the simulation data very closely, but there is significant variance in the off-axis responses, particularly in terms of the phase lag. Hence, for reasons of clarity, the phase plots are not presented.

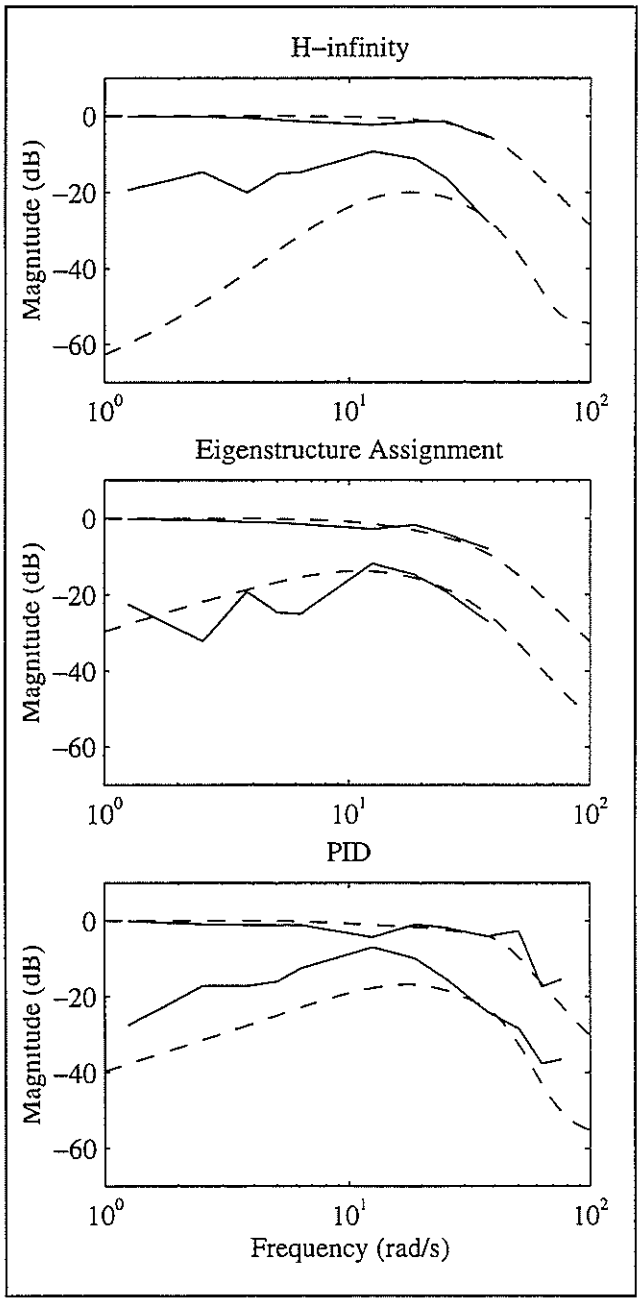

Figure 7
Comparison of experimental (solid) and modelled (dashed) attitude frequency response Bode magnitude for H_∞, Eigenstructure Assignment and PID closed-loop systems

The ratio of off-axis gain to on-axis gain at the -135 phase lag bandwidth frequency was -18.2dB for the H_∞ RSF closed-loop system, -16.4dB for the Eigenstructure Assignment RSF closed-loop system and -11.7dB for the PID rigid-body closed-loop system. It should also be noted that whilst the nominal performance of the H_∞ RSF closed-loop system is much superior, the experimental predictability of the Eigenstructure Assignment RSF closed-loop system is better.

The level of model uncertainty was the most significant problem encountered in implementing all the controllers on the Rotor Rig. For future work the fidelity of the flight mechanics design model needs to be refined to reduce the uncertainty, particularly of the coupled body rotor modes and the off-axis response. Individual blade element models with enhanced inflow dynamics are being investigated.

Comparison With Full-Scale

It has been shown that the fundamental character of coupled body/rotor behaviour for high bandwidth hingeless rotors is reproduced by the Rotor Rig, and that, *(i)* the normalised ratio of pitch/roll moments per unit flapping to rigid body inertia, *(ii)* the open-loop pitch/roll attitude bandwidths, and *(iii)* the level of model uncertainty, are all comparable with the Westland Lynx helicopter. Hence, in seeking to evaluate the closed-loop performance of the RSF controllers, it is valuable to relate the data back to full-scale.

Figure 9 presents the ADS-33D roll attitude bandwidth achieved or exceeded by both of the RSF closed-loop systems (scaled with respect to rotorspeed). Presented for comparison is the corresponding bandwidth calculated from flight test data for the DERA Lynx Mk. 7 for a similar hover flight condition.

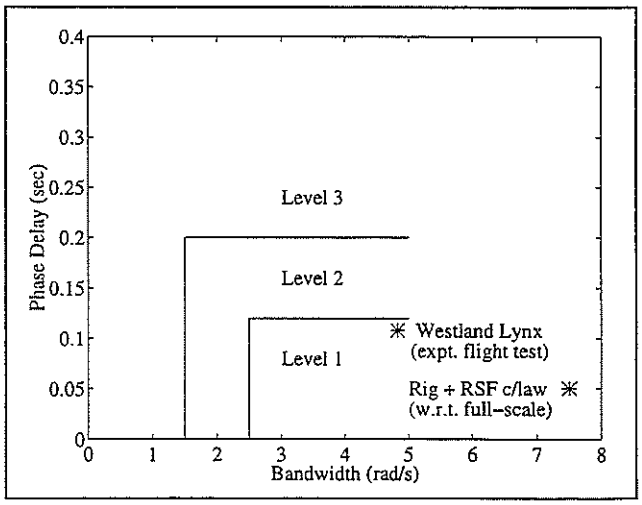

Figure 8
Comparison of Rig and Lynx roll attitude bandwidth

From this, it can be seen that an increase in closed-loop bandwidth of up to 50% (approx.) can be achieved. This comparison is not intended to demonstrate a Lynx-specific capability, but rather the level of robust performance improvement that could be attained for a stiff, hingeless rotor through application of RSF with respect to conventional limited authority, rigid-body feedback.

Overall, the concept of Rotor State Feedback would appear to yield potentially significant advances in robust, high bandwidth command tracking and disturbance rejection.

Conclusions

Previous study of controller design techniques has shown that Rotor State Feedback (RSF) controllers exhibit superior performance and robustness properties to single-input, single-output or multivariable rigid-body feedback controllers of similar structure. The experimental evaluation of RSF controllers on the University of Bristol Experimental Rotor Rig Facility has highlighted the following points :

- A simple mathematical proof has been stated that illustrates why robust, high bandwidth control requires RSF or sufficient dynamic compensation to estimate the rotor states.

- The Rotor Rig exhibits coupled body/rotor dynamics and model uncertainty representative of the Westland Lynx and provides a flexible environment for experimental testing of high bandwidth controllers.

- A detailed comparison of the implicit RSF properties of the output feedback H_∞ multivariable design technique and the explicit RSF properties of the full state feedback Eigenstructure Assignment multivariable design technique has been presented.

- Similar levels of performance and robustness have been achieved using both methods, but the full state feedback method allows greater design freedom in terms of retaining the classical modal dynamic behaviour.

- The experimental tests have included frequency sweeps and small, moderate and large amplitude step responses, with the results being related to full-scale in the context of ADS-33D flying qualities requirements.

- Up to a 50% increase in closed-loop bandwidth can be gained via RSF with respect to conventional limited authority rigid-body feedback

- Robust performance is maintained in the presence of 30% on-axis model uncertainty and 100% off-axis model uncertainty.

Future Work

The concept of RSF has been shown to yield potentially significant advances in robust, high bandwidth command tracking and disturbance rejection properties, but has also highlighted areas requiring further risk reduction :

- the integrity and fidelity of rotor state measurements need to be enhanced. A hub-mounted laser distance tranducer system has been tested at full-scale (Ref. 16), but a refined rotor blade strain-gauge assembly with additional hub-mounted signal conditioning remains the more viable route at model-scale.

- the fidelity of the flight mechanics design model needs to be refined to reduce the level of uncertainty, particularly of the coupled body rotor modes and the off-axis response. Individual blade element models with enhanced inflow dynamics are being investigated.

Further ahead, there are additional applications of RSF that need to be explored :

- whilst enhancing the overall capability to achieve robust, high bandwidth pilot-in-the-loop control, RSF would appear to have particular application to even higher bandwidth disturbance rejection/gust alleviation and the enhancement of ride qualities.

- the emergence of smart rotor technology also raises the potential for frequency splitting of the flight control input to the rotor system - e.g. large amplitude, low frequency rigid-body feedback ($\leq$ once per rev.) via the swashplate and small amplitude, high frequency RSF ($\geq$ once per. rev.) via the on-blade control surfaces. Whilst permitting control excitation at frequencies $\geq$ once per. rev., it also provides a level of redundancy not available with current technology.

Acknowledgement

This work was conducted under the auspices of the UK Ministry Of Defence and Department of Trade and Industry LINK Programme on "Enabling Technologies for Rotorcraft" and the Ministry Of Defence Corporate Research Item AS021Q14 "Rotor State Feedback".

References

1) Padfield, "An Initial Investigation into a Particular Form of Rotor State Feedback", Westland Helicopters Ltd. Research Memorandum 221, 1974.

2) Takahashi, "Rotor State Feedback in the Design of Flight Control Laws for a Hovering Helicopter", *Journal of the American Helicopter Society*, Vol. 39, No. 1, 1994.

3) Ham, "Helicopter Individual Blade Control : Promising Technology for the Future Helicopter", 21st European Rotorcraft Forum, 1995.

4) Anon, "Aeronautical Design Standard (ADS-33D) - Handling Qualities for Military Helicopters", US Army AVSCOM, 1994.

5) Brinson, "Experimental Investigation of Coupled Helicopter Rotor/Body Control", 17th European Rotorcraft Forum, 1991.

6) Curtiss Jr. and N.K. Shupe, "A Stability and Control Theory for Hingeless Rotors", 27th Annual Forum of the American Helicopter Society, 1971.

7) Padfield, Helicopter Flight Dynamics, Blackwell Science, 1996.

8) Tischler, "System Identification Requirements for High Bandwidth Rotorcraft Flight Control System Design", *AIAA Journal of Guidance, Control and Dynamics*, Vol. 13, No. 5, 1990.

9) Landis, J.M. Davis, C. Dabundo, J.F. Keller, "Advanced Flight Control Technology Achievements at Boeing Helicopters", *International Journal Of Control*, Vol. 59, No 1263-290, 1994.

10) Brinson, G.J. Mullen, J. Howitt and I.J. Woodrow, "Experimental Investigation of Control System Design Techniques for Helicopters", 21st European Rotorcraft Forum, 1995.

11) McFarlane and K. Glover, "A Loop Shaping Design Procedure Using H_∞ Synthesis", *IEEE Transactions on Automatic Control*, Vol. 37, No. 6, 1992.

12) Hyde, H_∞ Aerospace Control Design: A VSTOL Flight Application, Springer-Verlag Ltd., 1995.

13) Smerlas, I. Postlethwaite and D.J. Walker, "Full Envelope Robust Control Law for the Bell 205 Helicopter", 22nd European Rotorcraft Forum, 1996.

14) Andry, E.Y. Shapiro, and J.C. Chung, "Eigenstructure Assignment for Linear Systems", *IEEE Transactions on Aerospace and Electronic Systems*, September 1983.

15) O'Brien and J. Broussard, "Feedforward Control to Track the Output of a Forced Model", 17th IEEE Conference on Decision and Control, 1978.

16) Fletcher and M.B. Tischler, "Improving Helicopter Flight Mechanics Models with Laser Measurements of Blade Flapping", 53rd Annual Forum of the American Helicopter Society, 1997.